

Simulations of Hadron Calorimeter Segmentation for Electron Identification in the Compact Muon Solenoid

Tanner Prestegard
University of Minnesota

May 7, 2010

Abstract

The Compact Muon Solenoid (CMS) experiment is a particle detector on the Large Hadron Collider ring at CERN. Eventually, the LHC will receive a luminosity upgrade, in order to increase the rate of interesting discoveries. This luminosity upgrade will also increase pileup in the CMS detector. Segmentation of the hadron calorimeter of CMS into four energy readout groups has been proposed to improve signal purity under higher amounts of pileup. Simulations were done to identify optimal segmentations for electron identification in CMS. Along with possible layer segmentations, we explored different trigger tower geometries and “definitions” of the hadron calorimeter. The results indicate that layer segmentation is beneficial at high pileup numbers and that a 2x5 cluster geometry is the best option of those tested.

1 Introduction

The Compact Muon Solenoid (CMS) experiment is a particle detector designed to identify particles created in the proton-proton collisions produced by the Large Hadron Collider (LHC) at CERN. These collisions occur at center-of-mass energies of up to 14 TeV. The goals of the CMS experiment include the search for the Higgs boson, which is proposed to resolve electroweak symmetry breaking, as well as the exploration of physics beyond the Standard Model, like supersymmetry.

1.1 Detector Geometry and Components

The CMS detector is roughly cylindrical in shape, with the z -axis running parallel to the beam line. In the natural coordinate system of the detector, the azimuthal angle ϕ runs about the z -axis, in the

x - y plane, and the pseudorapidity η is measured relative to the beam axis. The pseudorapidity can be determined from the polar angle θ by

$$\eta = -\ln \left[\tan \left(\frac{\theta}{2} \right) \right].$$

These coordinates are used because it allows the origin to be placed at the point of collision for each beam crossing and because the pseudorapidity η is invariant under Lorentz transformations. There are three main regions of the detector: the barrel region and the two endcaps. This study is concerned with the barrel region of the detector.

This study focuses on the hadron calorimeter (HCAL) and, to a lesser extent, the electron calorimeter (ECAL) of the detector. A schematic of the detector with all components labeled can be seen in Figure 1. It is enough to know that the detector contains a solenoidal magnet that operates at 4 Tesla, as well as a silicon tracker, which determines the momentum of charged particles. The tracker calculates momentum based on the particle's deflection in the magnetic field at certain points in the detector. The tracker also determines the “track,” or path, of particles in the detector. The outermost region of the detector is designed to detect muons.

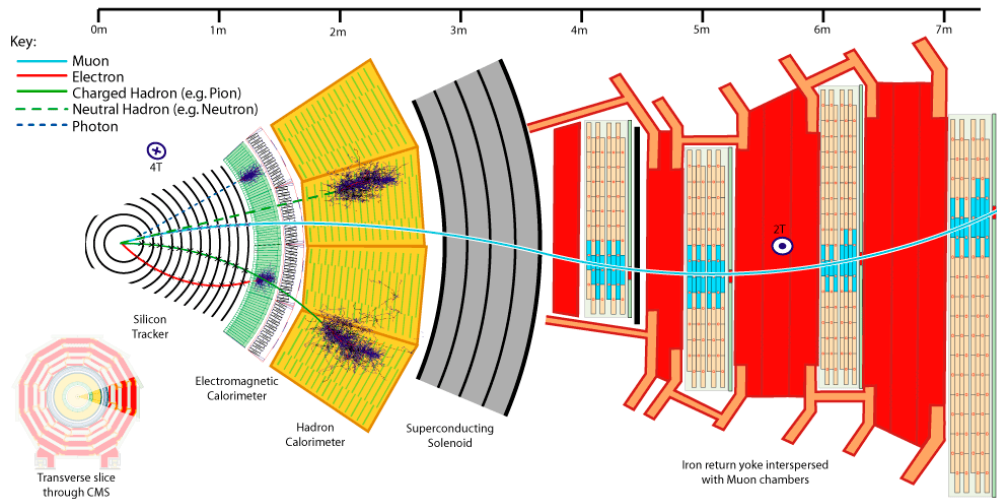


Figure 1: A slice of the CMS detector from a beam-axis perspective.

ECAL is composed of nearly 80000 scintillating lead tungstate crystals. It detects and measures the energies of electromagnetic particles through scintillation. In this process, an energetic particle excites

electrons in the medium it is traversing. When the electrons descend to their ground states, they emit an amount of light that is proportional to the energy of the traveling particle. ECAL measures the light output of the scintillators using photodetectors, which convert the emitted light into an electrical signal. Instead of dealing with individual crystal energies, this simulation focuses on arrays of crystals in ECAL, called trigger towers.

HCAL consists of alternating segments of plastic scintillator material and brass absorber. One scintillator tile and one absorber plate combine to form one layer in HCAL, and there are 17 HCAL layers in total. HCAL is designed to measure hadron energies as a sampling calorimeter. Collisions with the inactive absorber cause hadrons to lose energy, and the energy of the particles can be “sampled” in each scintillator tile. Like ECAL, HCAL is grouped into trigger towers for energy readout purposes. Currently, HCAL has a single photodetector per trigger tower for scintillation energy measurements.

1.2 SLHC Upgrade

As time goes on, the frequency of interesting discoveries made by a particle detector typically decreases. In order to combat these diminishing returns at detectors on the LHC ring, a luminosity upgrade to the LHC, called the Super Large Hadron Collider (SLHC), has been proposed. The luminosity of the SLHC is expected to be $10^{35} \text{ cm}^{-2}\text{s}^{-1}$, which is a factor of 10 increase from the LHC. Although a higher luminosity will allow for exploration of more areas of physics, it will also require adaptations of the data collection process.

Increased luminosity equates to more overall events, both interesting (signal) and uninteresting (background). However, it also leads to a phenomenon called “pileup,” which occurs when several particles affect the detector simultaneously, and causes particle identification to be particularly difficult. Pions constitute the main type of pileup produced by the proton-proton collisions from the LHC, and each pileup event produces about 50 charged pions and 50 neutral pions. Neutral pions interfere with calorimetry measurements due to their tendency to decay into two photons and produce an electron-like energy signal. Charged pions also interfere because they sometimes produce tracks in the detector. After the upgrade, the SLHC is expected to have about 40-50 pileup events per collision.

2 Experiment

2.1 Motivation

The goal of this study is to optimize electron identification and to minimize the survival rate of background particles in CMS at the SLHC. The primary impetus for this is the fact that electrons are often the decay products of interesting particles. It will be more difficult to identify interesting events in CMS at SLHC luminosities due to increased pileup. This precipitates the addition of more photodetectors for HCAL and an arrangement of them that optimizes their utility.

Another motivating cause is data storage limitations on offline computing systems [1]. Beam crossings in the CMS detector occur at a rate of 40 MHz (every 25 ns), however, the detector's triggering system retains only 100 events per second for data analysis. Because of this, it is important to properly identify events which contain results of interest.

The CMS triggering system has two components: the Level 1 Trigger System (L1) and the High Level Triggers (HLT). The Level 1 system filters the 40 MHz data rate to 100 kHz, and the HLT system filters the 100 kHz data rate to 100 Hz. This study is an analysis for the Level 1 system.

2.2 Approach

To better identify electrons in the CMS detector at increased pileup, division of the hadron calorimeter into multiple energy readout groups has been proposed. Currently, in the L1 trigger, the energy in all 17 layers of an HCAL trigger tower is summed for an event by a single photodetector. However, this practice provides no insight into how a particle's energy is distributed throughout HCAL. Electrons that pass through all of ECAL typically do not travel far into HCAL, while background particles may penetrate further and distribute their energy differently.

The proposed upgrade calls for the addition of three photodetectors per trigger tower, allowing for the division of HCAL into four energy readout groups, or "segments." Segmentation will provide increased information about a particle's depth of penetration and energy distribution in HCAL, which are important factors in particle identification. One energetic pion may have the same total energy as an event composed of a signal electron and multiple low-energy pions, but the single pion will likely deposit its energy deeper into HCAL. Segmentation will aid the trigger system in rejecting the first case and accepting the second. It will also allow for different definitions of HCAL to be explored.

To test the effectiveness of HCAL segmentation, a simulation of signal and background events in the CMS detector was performed. This simulation employed four possible arrangements of the 17 HCAL layers, in addition to the current readout setup. The current setup, along with the four segmentation options tested in this simulation, can be seen in Figure 2.

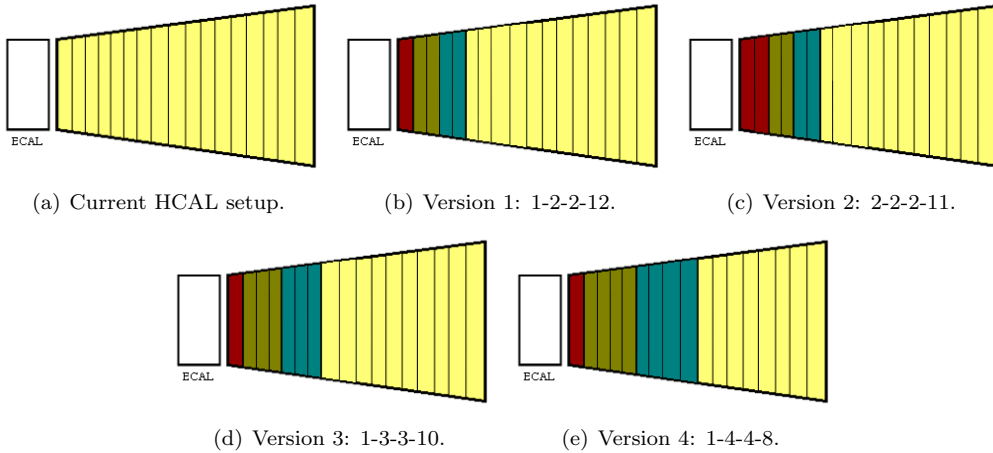


Figure 2: HCAL segmentations considered in this simulation for the SLHC upgrade. The segments are grouped by color.

Three other parameters were also considered in this simulation: ECAL purity, cluster geometry, and HCAL “definitions.” ECAL purity is given by

$$ECAL\ Purity = \frac{E_{ECAL}}{E_{ECAL} + E_{HCAL}}. \quad (1)$$

Here, E_{ECAL} is the total energy deposited in the electromagnetic calorimeter, and E_{HCAL} is the total energy deposited in the hadron calorimeter. ECAL purity is a useful parameter in this study because electrons are expected to deposit nearly all of their energy in ECAL, and thus have high ECAL purity. The ECAL purity of typical background particles is expected to be much lower. For this reason, ECAL purity was used to make signal and background survival cuts in this simulation.

In the CMS detector, a cluster is defined as a group of trigger towers. When an event occurs in CMS, the trigger tower in ECAL with the most energy deposited in it is defined as the seed. A cluster geometry is a pre-defined arrangement of trigger towers around the seed tower, and includes towers in both ECAL and HCAL. In this simulation, a 2x3 cluster geometry and a 2x5 cluster geometry were considered. A 2x3 cluster geometry refers to a two-tower array in ECAL, consisting of the seed tower

and its highest-energy neighbor, and a 3x3 array of towers in all layers of HCAL. The HCAL tower array is situated directly behind the ECAL seed tower. The 2x5 cluster geometry is identical to the 2x3, apart from the fact that it features a 5x5 array of towers in HCAL, instead of a 3x3 array. The choice of cluster geometry defines which trigger tower energies are included in the total ECAL energy and in the total HCAL energy for an event; thus it is an inherent attribute of ECAL purity.

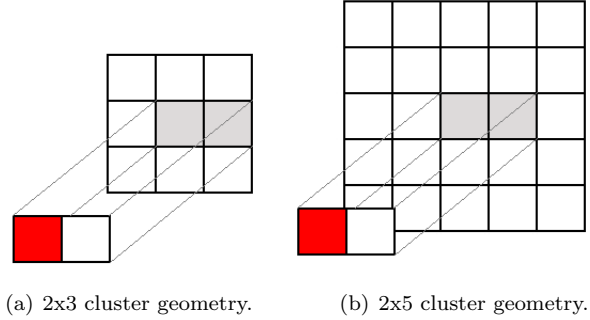


Figure 3: Cluster geometries tested in this simulation. ECAL towers are pictured in the foreground, while HCAL towers are shown in the background. The ECAL seed tower is shown in red.

We also considered different definitions of a final energy readout for HCAL. All of the segmentation options shown in Figure 2 have Segment 1 of HCAL defined as only 1 or 2 layers. Energetic electrons that pass through all of ECAL will likely deposit their remaining energy in the first few layers of HCAL, while hadronic background particles will deposit their energy throughout all of HCAL. Thus, completely ignoring the energy in the first segment of HCAL could give a very high ECAL purity (as shown in Equation 1) for electrons, and a lower ECAL purity for background. More information about the specific HCAL definitions used in this simulation is given in Table 1.

HCAL Definition	HCAL Segments Included
All	Segments 1,2,3,4 (current setup)
234	Segments 2,3,4
34	Segments 3,4
Hybrid	Segments 1,2,3,4 ¹

Table 1: HCAL definitions explored in this simulation and their respective segments whose energy is included in E_{HCAL} .

¹A hybrid HCAL definition with a 2x3 cluster geometry consists of two towers in ECAL, two towers in Segment 1 of HCAL, and a 3x3 array of towers in Segments 2-4 of HCAL. The 2x5 hybrid definition is analogous, with a 5x5 array of towers in Segments 2-4 of HCAL.

2.3 Simulation

A simulated version of the detector has been constructed in the CMSSW software and is being used to test the effects of HCAL segmentation on the identification of electrons by the CMS detector at the SLHC. This simulation was done in CMSSW 2.2.5, and the analysis was done in CMSSW 2.2.11. Two simulated collision types were chosen to represent possible scenarios in the detector.

A dielectron simulation was selected to represent generation of pure signal particles. In this simulation, each event produces two electrons that travel in opposite directions in ϕ -space. The electrons have a flat energy distribution, which ranges from 20-120 GeV. The position distribution of the electrons in η -space and ϕ -space is also flat along the entire barrel. This simulation is considered to be nonphysical because the electrons are not created by an actual decay process; they are generated spontaneously. Thus, these simulated events have no real cross section. The cross section used for the signal particles is based on the cross section of Z-boson decay ($Z \rightarrow e^- + e^+$) at 10 TeV, which is 2.340 pb.

Background particles in this simulation were represented by QCD dijet events. A QCD jet is a narrow cone of particles that is created by hadronization of quarks and gluons that were freed or created by the proton-proton collisions from the LHC. The QCD dijets in this simulation are divided into two transverse energy bins, due to cross sections that vary with energy. The two bins are 40-180 GeV and 180-400 GeV. The low energy and high energy QCD bins have cross sections of 6.3×10^7 pb and 1.0×10^5 pb, respectively.

2.4 Simulation Triggering Algorithms

A typical electron deposits 97% of its energy within a single trigger tower in ECAL [1]. Such a tower is called a seed. An electron seed is primarily identified in the detector by an electron-photon triggering method in the detector, which has been replicated in this simulation. Due to the presence of the magnetic field of the detector solenoid, the trajectories of electrons and photons are curved in ϕ -space. Hence, we expect that electron showers will spread in ϕ . To improve background rejection at the ECAL level, the detector employs a triggering system to identify electrons and photons by this behavior. In this simulation, the analysis algorithm divides each ECAL trigger tower into five strips, each 1 crystal in η and 5 crystals in ϕ . The energy in each pair of adjacent strips is summed to find the maximum dual-strip energy value, as shown in Figure 4.

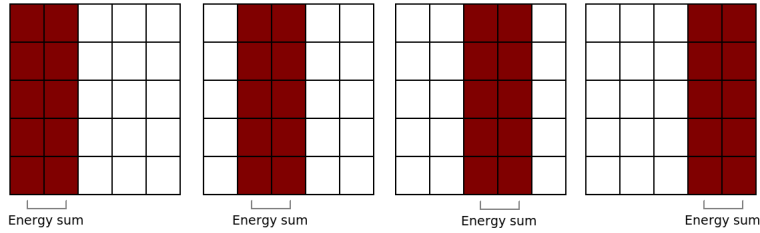


Figure 4: Electron-photon triggering algorithm being applied to an ECAL trigger tower.

If the ratio of this value to the energy of the entire trigger tower does not exceed a set parameter R , the trigger tower is rejected as a candidate for the seed of an electron. To match the specifications of the detector, we selected $R = 0.9$ [2].

3 Results

Figure 5 shows the current detector performance with no HCAL segmentation at 20 pileup, typical of the current LHC luminosity. Here, the two energy bins of the QCD dijet background have been weighted according to their cross-sections and combined into a total QCD background.

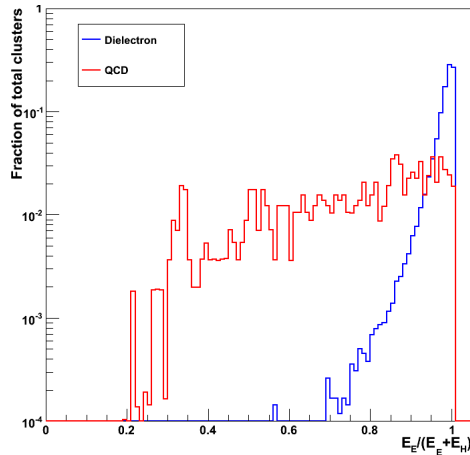


Figure 5: A plot of the fraction of total events vs. ECAL purity at 20 pileup and no HCAL segmentation, with a 2x5 cluster geometry.

Note that the dielectron signal has a much higher fraction of events at or near 100% ECAL purity than the background. This fraction decreases at higher pileup, making the signal harder to discern from the background. This effect can be seen in Figure 6.

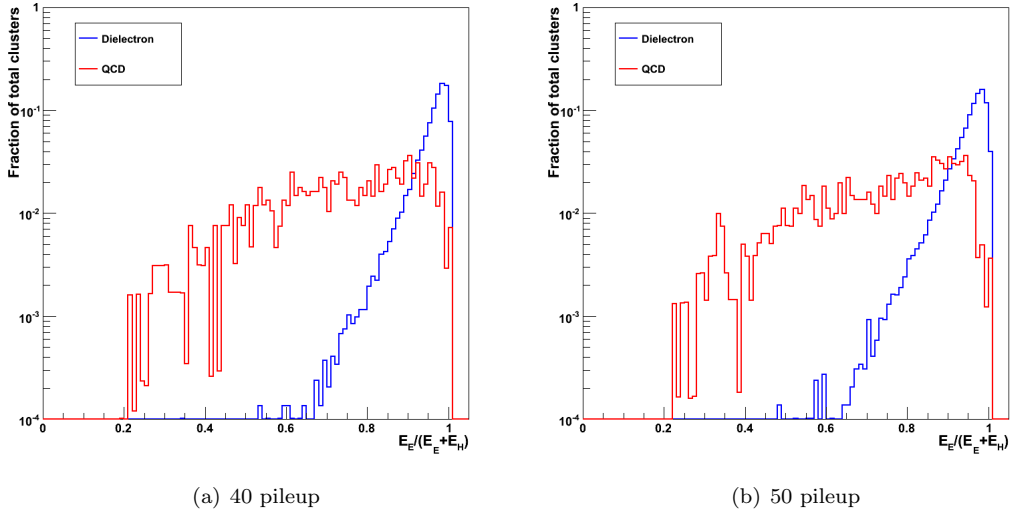


Figure 6: Plots of the fraction of total events vs. ECAL purity at higher pileup numbers and no HCAL segmentation, with a 2x5 cluster geometry. These plots simulate the current detector performance at SLHC-like pileup numbers.

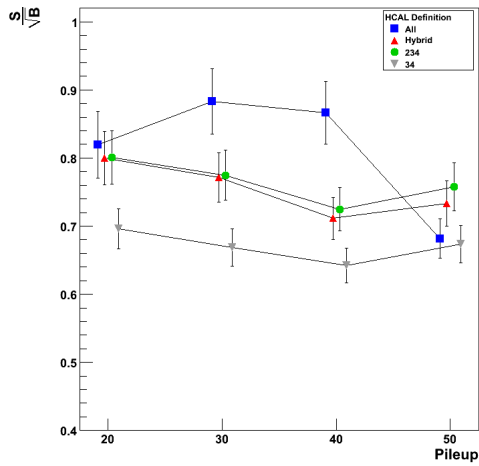
A more interesting way to look at the data is to integrate these plots over ECAL purity, in order to get signal and background “survival” rates as a function of ECAL purity. This shows the fraction of all signal events and the fraction of all background events that have passed an arbitrary ECAL purity cut. With this, however, it is also possible to work with signal survival as a function of background survival, and vice versa. This is optimal because the primary consideration is not absolute signal survival, but signal survival relative to background survival.

The ultimate results of this simulation are presented in terms of $\frac{S}{\sqrt{B}}$, where S is the signal and B is the background. In Poisson statistics, the uncertainty on a random variable X is equivalent to \sqrt{X} . Thus, maximizing $\frac{S}{\sqrt{B}}$ optimizes the signal with respect to fluctuations in the background. This approach is useful when searching for new particles.

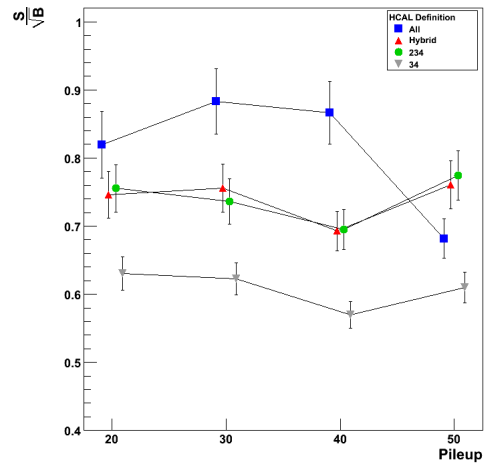
The following results are at a constant integrated luminosity of $1 fb^{-1}$, or $10^3 pb^{-1}$. Data have been compiled for signal survival rates of 85%, 95%, and 98%. These values span the range from what is typically considered low signal survival to high signal survival. All plots shown are in terms of $\frac{S}{\sqrt{B}}$ relative to what is considered a clean signal (2 pileup) with the current HCAL readout setup².

Figure 7 shows results for the 2x5 cluster geometry at 85% signal efficiency.

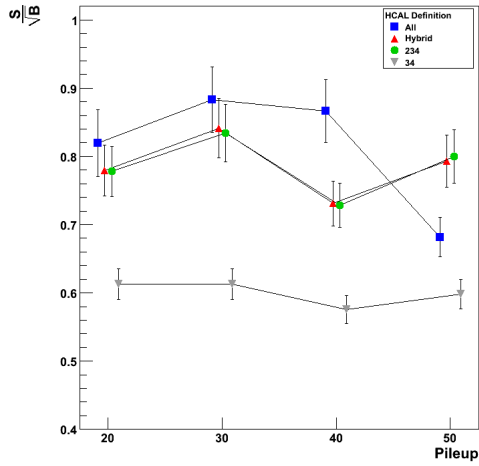
²For all $\frac{S}{\sqrt{B}}$ plots shown in this section, all data points occur at the pileup values shown on the x-axis (20, 30, 40, and 50). Some of the series have been adjusted horizontally for the ease of the reader.



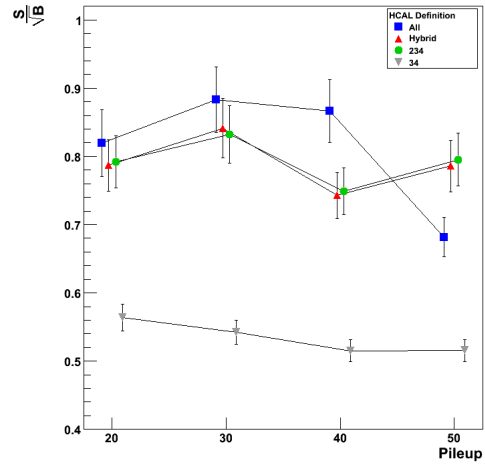
(a) Version 1.



(b) Version 2.



(c) Version 3.



(d) Version 4.

Figure 7: Versions 1-4 at 85% signal efficiency with a 2x5 cluster geometry. Uncertainties shown are relative. Absolute uncertainties are approximately 0.06.

In Figure 7, the ALL HCAL definition corresponds to the current readout setup. At 50 pileup, the effectiveness of this setup decreases significantly, and the 234 and hybrid definitions surpass it. One would expect this trend to continue with increasing pileup. The 34 definition does not perform very well, especially in Versions 3 and 4.

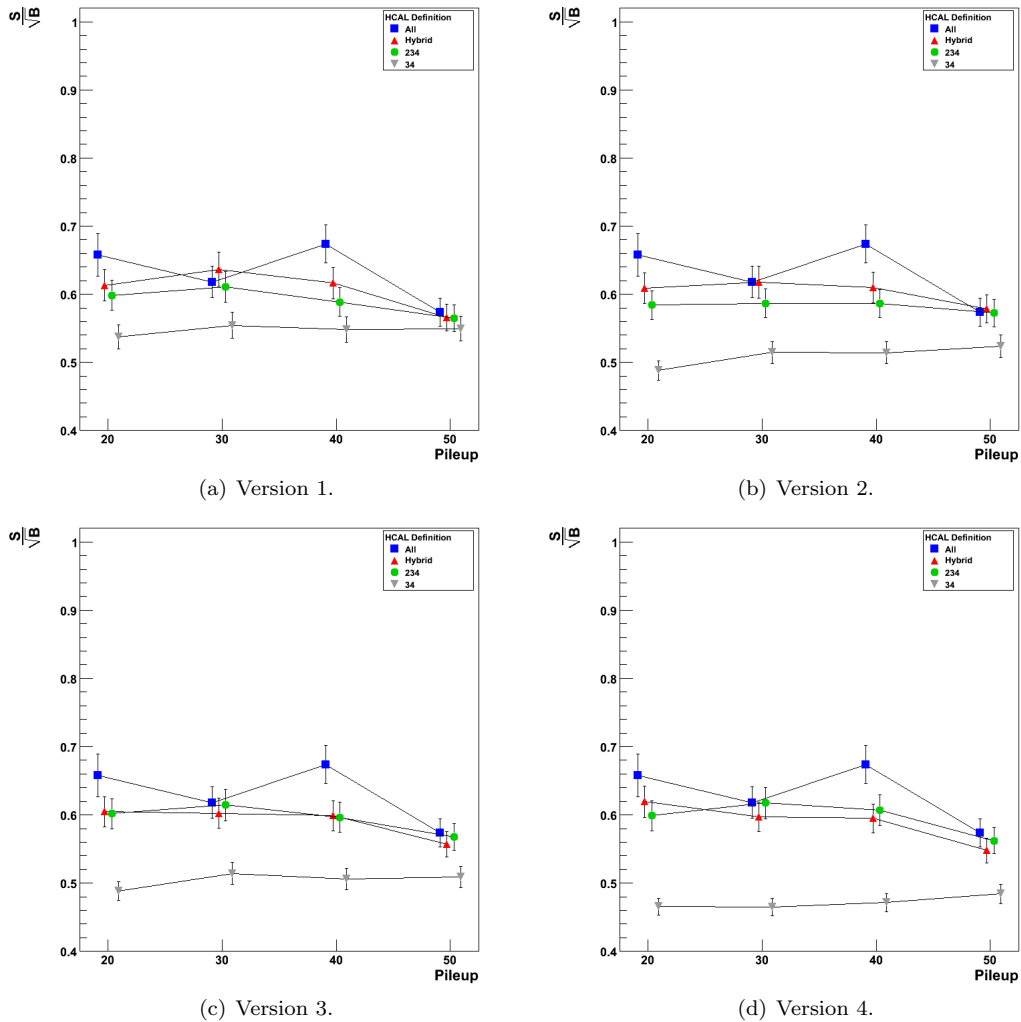


Figure 8: Versions 1-4 at 85% signal efficiency with a 2x3 cluster geometry. Uncertainties shown are relative. Absolute uncertainties are approximately 0.06.

The 2x3 cluster geometry shown in Figure 8 produces lower $\frac{S}{\sqrt{B}}$ values compared to the corresponding 2x5 cluster geometry values shown in Figure 7. It is likely that this is related to the lateral spread of the background events in the detector and how that manifests itself in the cluster geometry and in the ECAL purity cut. It is also not clear that segmentation is beneficial for the 2x3 cluster geometry.

However, the 2x5 cluster geometry outperforms the 2x3 cluster geometry in all variations of segmentation and signal efficiency. Thus, results will be presented only for the 2x5 geometry for 95% and 98% signal efficiency. Plots for these efficiencies can be seen in Figure 9 and Figure 10. Refer to the

appendix for plots of the 2x3 cluster geometry at 95% and 98% signal efficiencies.

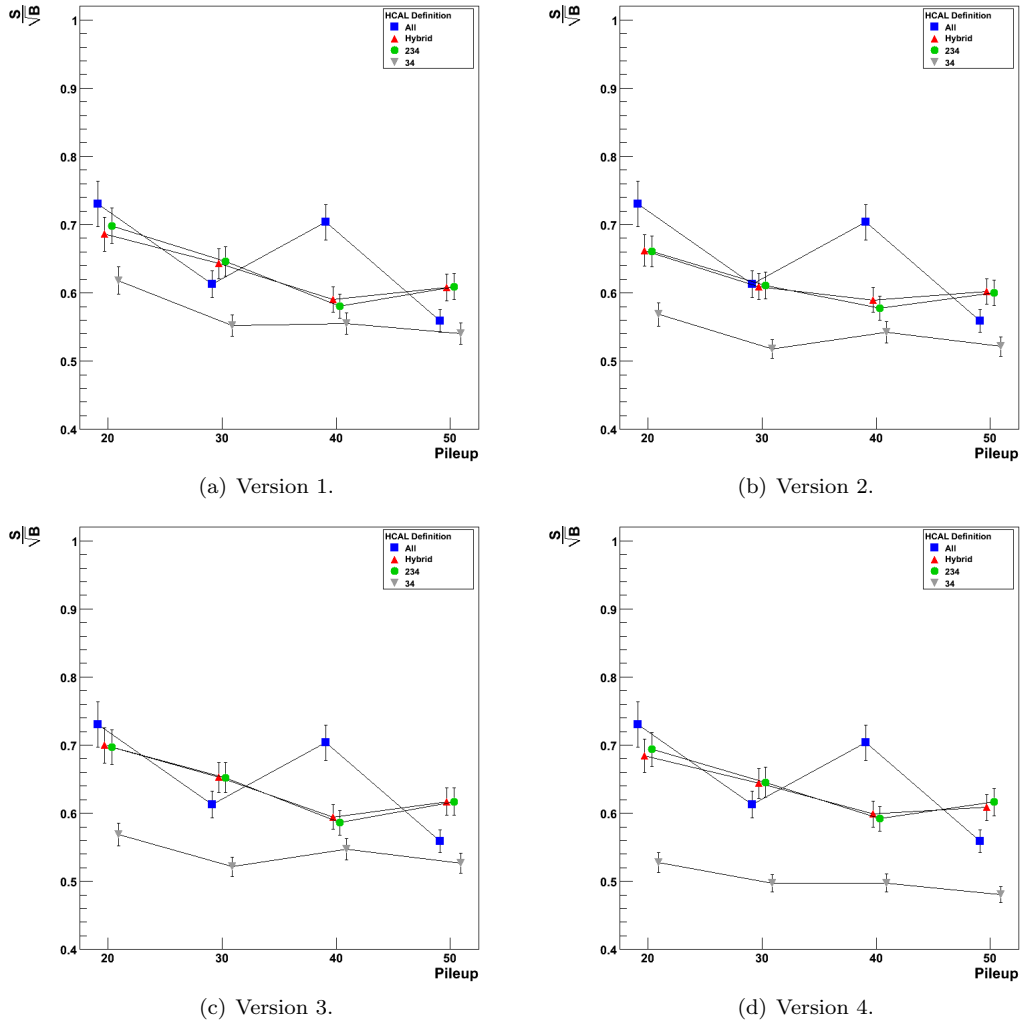
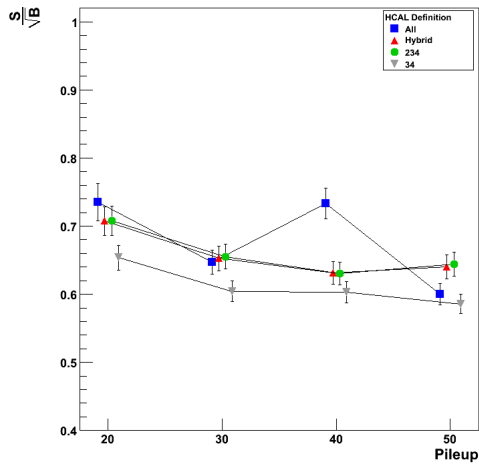
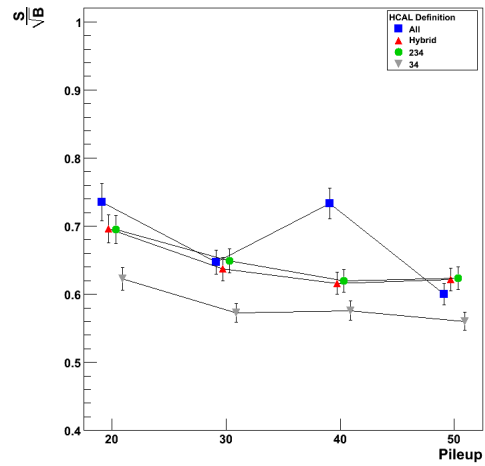


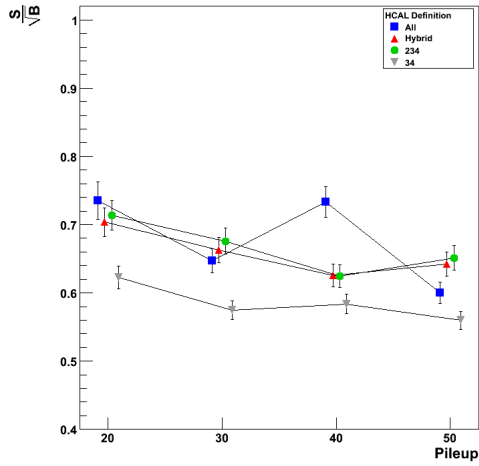
Figure 9: Versions 1-4 at 95% signal efficiency with a 2x5 cluster geometry. Uncertainties shown are relative. Absolute uncertainties are approximately 0.05.



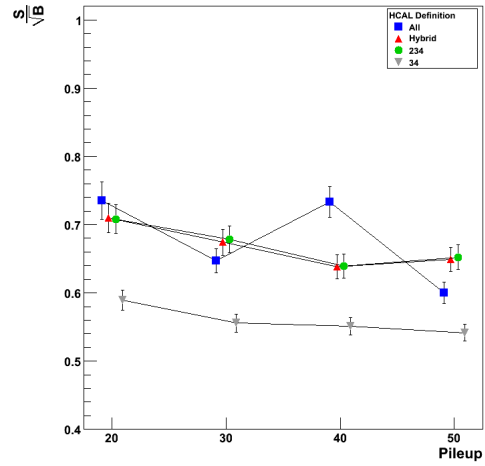
(a) Version 1.



(b) Version 2.



(c) Version 3.



(d) Version 4.

Figure 10: Versions 1-4 at 98% signal efficiency with a 2x5 cluster geometry. Uncertainties shown are relative. Absolute uncertainties are approximately 0.04.

Most of the trends that were seen at 85% signal efficiency are also evident at 95% and 98% signal efficiency. The hybrid and 234 definitions perform the best at 50 pileup, and it is not possible to conclude which is superior. The 34 definition still appears to be the least effective, but less drastically so for increased signal efficiency. Something interesting to note in Figures 9 and 10 is how the ALL definition behaves rather strangely at 30 pileup.

4 Conclusions

Overall, it is clear that segmentation of the hadron calorimeter has a beneficial effect on electron identification in CMS at pileup numbers expected from the SLHC. The effectiveness of the current HCAL energy readout setup decreases significantly at 50 pileup, while the 234 and hybrid definitions provide better signal identification. At this point, it is not clear which segmentation version is optimal, although an increasing trend can be noted as the version number increases. Increasing version number corresponds to an increasing number of layers in segments 2 and 3 of HCAL. However, this is something to note, and certainly not a definite conclusion.

It is difficult to say whether the 234 definition or the hybrid definition performs better at high pileup. However, it is evident that the 2x5 cluster geometry produces results superior to that of the 2x3 cluster geometry and that the 34 HCAL definition is the least effective definition. Both of these statements hold true for all segmentation versions at all signal efficiencies.

This simulation does have some limitations which should be considered. The first limitation is related to the CMSSW software: the responses of the simulated ECAL and HCAL were not completely tuned to the specifications of the actual detector until more recent versions of the software. It is not clear at the present time how this change in response would affect the results presented here.

Secondly, the energy sensitivity of HCAL is limited. While photons produced by neutral pion decay are typically measured by ECAL, charged pions can sometimes exchange a quark with the HCAL absorber material. This creates a neutral pion, which decays into photons that are absorbed in HCAL. Limits on energy sensitivity in HCAL may not allow this energy to be recorded. This effect may be related to the unexpected similarity of the hybrid and 234 HCAL definitions.

Lastly, results from recent 7 TeV collisions in the CMS detector indicate that there are more particles being produced from pileup than predicted in this simulation. There are approximately 4 times more particles being produced in each pileup event than expected, including 1 particle with at least 1 GeV of transverse energy, which is non-negligible. We expect this effect to be even more pronounced at the eventual collision energy of 14 TeV.

Based on these limitations, it would be useful to perform the simulation with a newer version of this CMSSW software in order to account for the updated ECAL and HCAL responses and the unexpected number of particles. Eventually, these results, along with those of other analyses, will influence the

segmentation of the HCAL energy readout system of CMS for the SLHC luminosity upgrade.

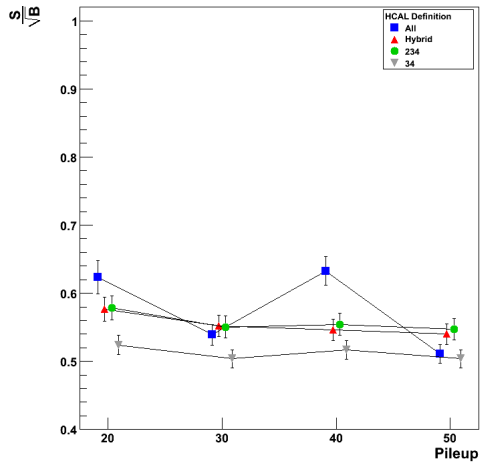
Acknowledgments

I would like to thank my advisor, Dr. Jeremy Mans, for his guidance and instruction on this project. I would also like to thank Aaron Feickert, an REU student from North Dakota State University, who wrote a significant amount of the code that this project was based on. Lastly, I would like to thank Bryan Dahmes, a postdoc in our group, who assisted me at various times during the course of this research.

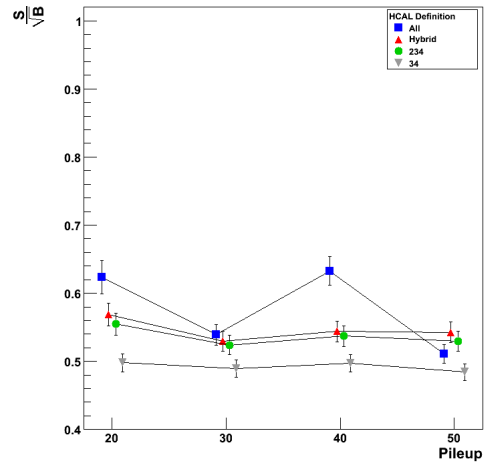
References

- [1] CMS Collaboration. *CMS: The TriDAS Project. Technical Design Report, Volume 1: The Trigger Systems*. CERN, 2000.
- [2] CMS Collaboration. *CMS Physics: Technical Design Report. Volume 1: Detector Performance and Software*. CERN, 2006.

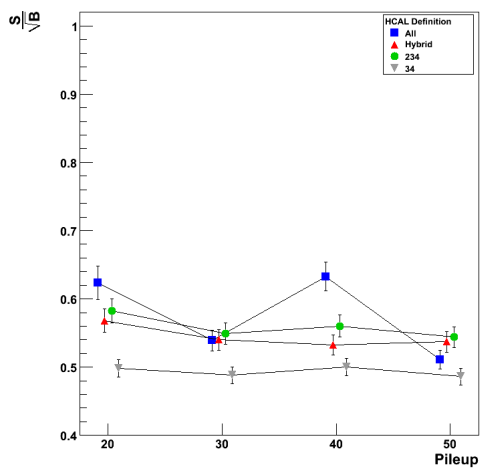
A Complete Data



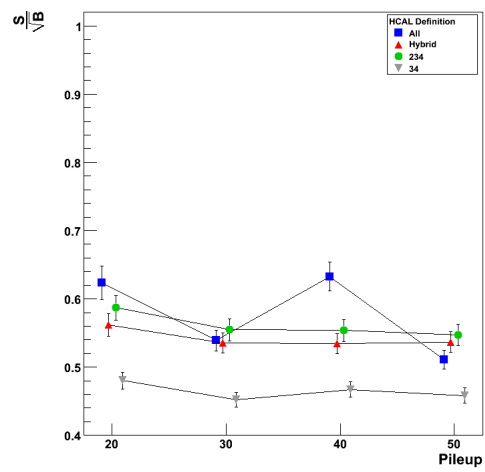
(a) Version 1.



(b) Version 2.

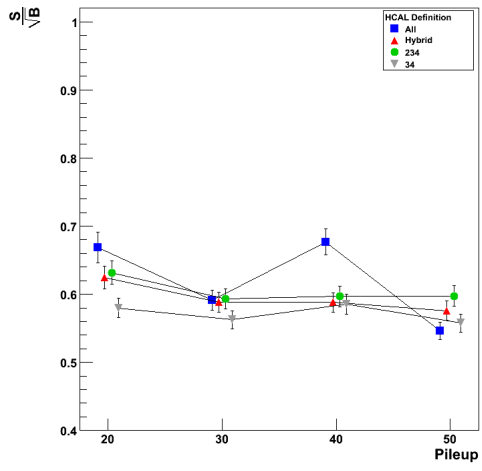


(c) Version 3.

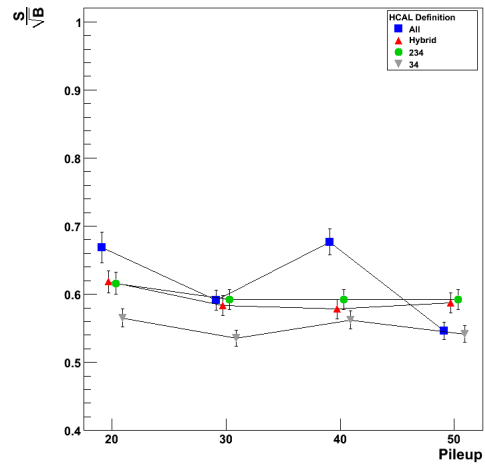


(d) Version 4.

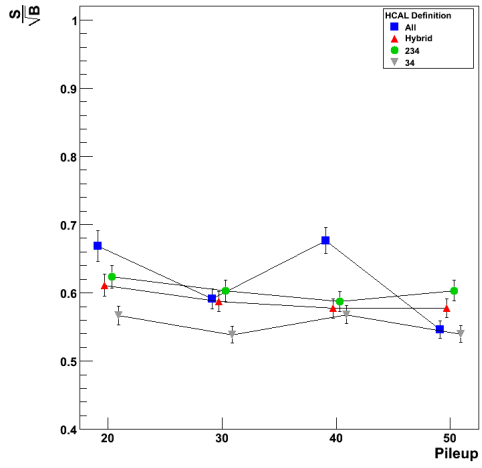
Figure 11: Versions 1-4 at 95% signal efficiency with a 2x3 cluster geometry.



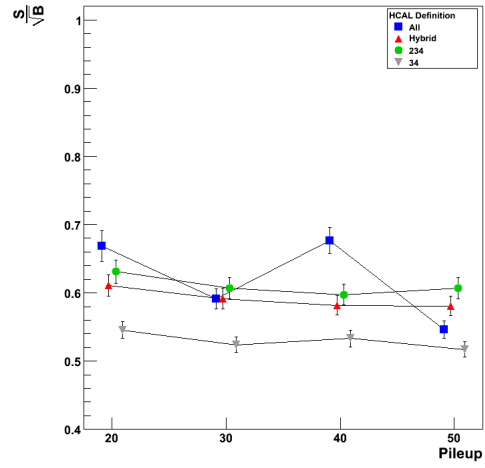
(a) Version 1.



(b) Version 2.

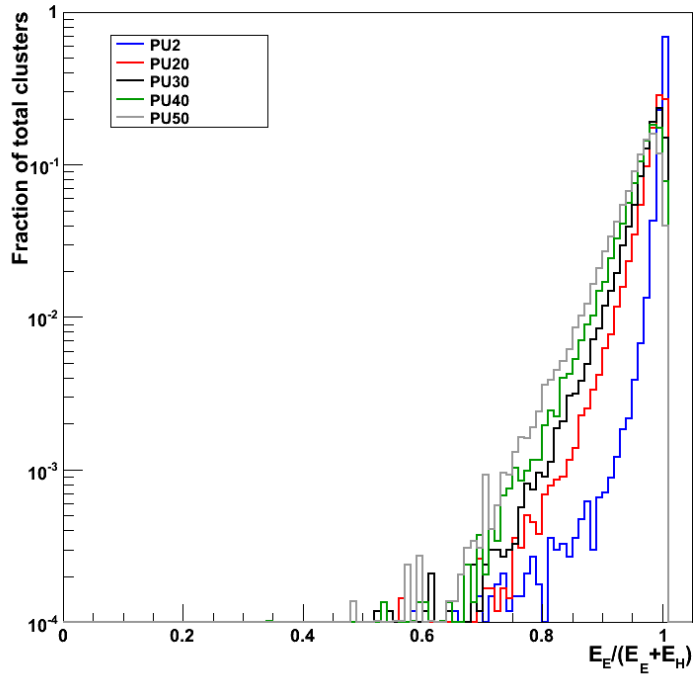


(c) Version 3.

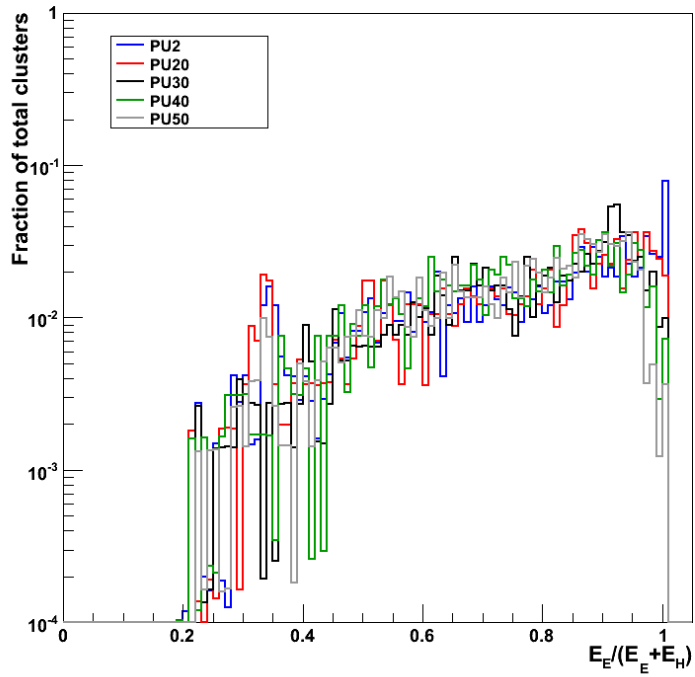


(d) Version 4.

Figure 12: Versions 1-4 at 98% signal efficiency with a 2x3 cluster geometry.



(a) Dielectron signal.



(b) QCD background.

Figure 13: Effect of pileup on ECAL purity of signal and background.